Zygote

cambridge.org/zyg

Exosc10 deficiency in the initial segment is dispensable for sperm maturation and male fertility in mice

Meiyang Zhou[#], Junjie Yu[#], Yu Xu, Hong Li, Yan-Qin Feng, Xiao Wang, Fanyi Qiu, Nana Li and Zhengpin Wang

Shandong Provincial Key Laboratory of Animal Cell and Developmental Biology, School of Life Sciences, Shandong University, Qingdao 266237, PR China

Research Articles

Cite this article: Zhou M *et al*. (2024) *Exosc10* deficiency in the initial segment is dispensable for sperm maturation and male fertility in mice. *Zygote*. **32**: 437–445. doi: 10.1017/S0967199424000418

Received: 10 March 2024
Accepted: 18 October 2024
First published online: 18 November 2024

Keywords:
epididymis; EXOSC10; initial segment; spermatogenesis; sperm maturation

Corresponding author:
Zhengpin Wang;
Email: zhengpin.wang@sdu.edu.cn or Nana Li;
Email: 202390900042@sdu.edu.cn

[#]These authors contributed equally to this work

Summary

EXOSC10 is an exosome-associated ribonuclease that degrades and processes a wide range of transcripts in the nucleus. The initial segment (IS) of the epididymis is crucial for sperm transport and maturation in mice by affecting the absorption and secretion that is required for male fertility. However, the role of EXOSC10 ribonuclease-mediated RNA metabolism within the IS in the regulation of gene expression and sperm maturation remains unknown. Herein, we established an *Exosc10* conditional knockout (*Exosc10* cKO) mouse model by crossing *Exosc10*$^{F/F}$ mice with *Lcn9-Cre* mice which expressed recombinase in the principal cells of IS as early as post-natal day 17. Morphological and histological analyses revealed that *Exosc10* cKO males had normal spermatogenesis and development of IS. Moreover, the sperm concentration, morphology, motility, and frequency of acrosome reactions in the cauda epididymides of *Exosc10* cKO mice were comparable with those of control mice. Thus, *Exosc10* cKO males had normal fertility. Collectively, our genetic mouse model and findings demonstrate that loss of EXOSC10 in the IS of epididymis is dispensable for sperm maturation and male fertility.

Introduction

In rodents, spermatozoa undergo a series of modifications to gain motility and maturity, and to acquire their capacity to fertilize ova during transit through the epididymis. The epididymis is a convoluted reproductive organ divided into four unique anatomical regions, including initial segment (IS), caput (CAP), corpus (COR), and cauda (CAU) (Cosentino and Cockett 1986; Elbashir *et al.*, 2021; Zhou *et al.*, 2018). Each region consists of distinct cell types that synthesize and secrete specific proteins and possess distinct transcriptome that plays different physiological functions in the maturation, concentration, and storage of sperm (Dube *et al.*, 2007; Johnston *et al.*, 2005; Thimon *et al.*, 2007). The epididymal epithelium is mainly comprised of principal, basal, apical, clear, halo, and narrow cells found only in the IS (Joseph *et al.*, 2011; Martinez-Garcia *et al.*, 1995; Sullivan *et al.*, 2019). These distinct cell types constitute a region-specific luminal microenvironment needed for sperm transport, concentration, and maturation (Cornwall 2009; James *et al.*, 2020).

The IS has a wide luminal diameter lined by elongated epithelial cells containing stereocilia. Reportedly, the epithelial cells of IS absorb ~90% of the fluid to concentrate the sperm during transition (James *et al.*, 2020). According to previous studies, defects in IS formation and differentiation adversely affect sperm maturation and male fertility (Krutskikh *et al.*, 2011; O'Hara *et al.*, 2011; Sipila *et al.*, 2002; Sonnenberg-Riethmacher *et al.*, 1996). Thus, investigating the IS functions during spermatozoa transition and maturation in the epididymis will provide molecular insights into the mechanisms underlying male fertility in mammals.

EXOSC10, an important ribonuclease associated with the RNA exosome complex, degrades and processes a wide range of nuclear transcripts through its enzymatic activities (Knight *et al.*, 2016; Pefanis *et al.*, 2015; van Dijk *et al.*, 2007). Mutations in RNA exosome-related genes are related to various diseases, including myeloma, diarrhea, and neurodegenerative disorders (Hartley *et al.*, 2010; Rudnik-Schöneborn *et al.*, 2013; Weißbach *et al.*, 2015). Recently, EXOSC10 has been reported to regulate gamete development in mice. Specifically, it promotes the maturation of mouse oocytes by modulating the transcriptome to degrade the growth-phase factors encoding RNAs (Wu and Dean 2020). Additionally, EXOSC10 controls the onset of spermatogenesis in male germ cells (Jamin *et al.*, 2017); however, the role of EXOSC10 ribonuclease-mediated RNA metabolism within the IS in the regulation of gene expression and sperm maturation remains unclear.

In this study, we established an *Exosc10* conditional knockout mouse (*Exosc10* cKO) model by crossing *Exosc10*$^{F/F}$ mice with *Lcn9-Cre* mice that expressed the recombinase in the principal cells of IS as early as post-natal day 17 (P17) (Gong *et al.*, 2021). Histological analysis revealed

that *Exosc10* cKO males had normal spermatogenesis and development of the IS of the epididymis. Moreover, cauda epididymis of *Exosc10* cKO males showed normal sperm abundance, morphology, motility, and spontaneous acrosome reaction frequencies comparable with those of control mice. Thus, the fertility test showed that *Exosc10* cKO males had normal fertility. Collectively, these results demonstrate that EXOSC10 deficiency in the IS of the epididymis does not affect sperm development, maturation, motility, or male fertility.

Materials and methods

Animals

All the animal procedures were approved by the Ethics Committee for Animal Research of the School of Life Sciences, Shandong University, China, and were performed according to the guidelines for the care and use of laboratory animals. *Exosc10*$^{F/F}$ mice were purchased from Cyagen. The *Lcn9-Cre* mouse line was provided by Professor Xiao-Yang Sun (Gong *et al.*, 2021).

Mouse genotyping

Mouse tails were lysed in DirectPCR Lysis Buffer with proteinase K at 56 °C overnight, followed by incubation at 85 °C for 1 h to inactivate proteinase K. High-Fidelity PCR Mix (RiboBio Co., LTD) and primers were used to amplify specific DNA fragments. PCR reaction employed an annealing temperature of 58 °C for 35 cycles using Mastercycler Pro (Eppendorf). Genotyping primers are listed in Supplementary Table S1.

Fertility assay

To assess male fertility, control or *Exosc10* cKO males were co-caged with wild-type female mice for at least 3 months. The average number of pups per litter was recorded and at least 3 mating cages were set up for each genotype.

Histological analysis

Mouse testes and epididymides were fixed in Bouin's solution and 4% paraformaldehyde (PFA) overnight at 4 °C for histological analysis and immunostaining, respectively. Samples were embedded in paraffin and cut into 5 μm thick sections, followed by staining with hematoxylin and eosin (H&E). The sperm from cauda epididymis were spread onto slides, air-dried overnight, and fixed with 4% PFA in phosphate-buffered saline (PBS) for 30 min, followed by staining with H&E.

Immunofluorescence

After de-waxing, rehydration, and antigen retrieval with 0.01% sodium citrate buffer (pH 6.0), sections were immersed in blocking buffer containing 0.05% Tween-20 at RT for 1 h and incubated with primary antibodies (Supplementary Table S2) overnight at 4 °C. Specific secondary antibodies (Supplementary Table S2) were used to detect the antigen, and DNA was stained with Hoechst 33342. Brightfield and fluorescent images were captured with a fluorescent microscope (Nexcope NE950).

Immunoblot assay

Total protein extraction utilized 1x LDS sample buffer and 1x NuPAGE sample reducing agent (Thermo Fisher Scientific). The extracted proteins were separated on 4–12% Bis-Tris gels and transferred to polyvinylidene fluoride membranes. The membranes were blocked with 5% non-fat milk in Tris-buffered saline containing 0.05% Tween-20 (TBST) for 1 h at RT and incubated overnight with primary antibodies (Supplementary Table S2) at 4 °C. Subsequently, the membranes were washed with TBST and incubated with secondary antibodies (Supplementary Table S2) for 1 h at RT. Thereafter, the membranes were washed with TBST and developed using SuperSignal West Dura Extended Duration Substrate (Thermo Fisher Scientific). Finally, the signals were detected with Hyperfilm ECL (GE Healthcare) according to the manufacturer's instructions.

RNA isolation and quantitative real-time RT-PCR

Total RNA was extracted from the IS of mouse epididymides using AFTSpin Tissue/Cell Fast RNA Extraction Kit for Animal (ABclonal) and cDNA was synthesized with ABScript III RT Master Mix (ABclonal). Quantitative RT-PCR was performed using Universal SYBR Green Fast qPCR Mix (ABclonal) and the QuantStudio 6 Flex Real-Time PCR System (Thermo Fisher Scientific). The primers are listed in Supplementary Table S1. The relative abundance of each transcript was calculated by $2^{-\Delta\Delta Ct}$ and normalized to endogenous *β-actin* expression (Livak and Schmittgen 2001).

Computer-assisted sperm analysis

Cauda epididymides were isolated from adult mice and cut into pieces in 500 μl M2 medium (Sigma-Aldrich). Sperm were released for 10 or 120 min at 37 °C under 5% CO_2. Then, 10 μl of sperm fluid was put into a glass cell chamber and observed through a 20X objective lens. The sperm concentration and motility were analyzed using computer-assisted sperm analysis (CASA). At least 200 sperm per mouse were analyzed and experiments were repeated thrice.

Spontaneous acrosome reaction

Sperm collected from cauda epididymides were incubated in TYH medium at 37 °C under 5% CO_2 for 1 h. Both non-capacitated and capacitated sperm were spread onto slides and air-dried, followed by fixation with 4% PFA for 15 min, washing with PBS, and staining with FITC-conjugated *Arachis Hypogaea* (peanut) agglutinin (PNA, 15 μg/ml) at 37 °C for 1 h. Simultaneously, the sperm nuclei were stained with Hoechst 33342 and images were captured with a fluorescent microscope (Nexcope NE950). Spontaneous acrosome reaction frequency was calculated by the ratio of PNA-negative sperm to Hoechst 33342-positive sperm. At least 200 sperm per mouse were analyzed and repeated thrice.

Statistical analysis

Statistical analysis was performed using GraphPad Prism. The variances of the two groups were compared by the two-tailed Student's t-test, and significance was defined as ns, no significance, $^{*}P < 0.05$, $^{**}P < 0.01$, $^{***}P < 0.001$, and $^{****}P < 0.0001$.

Results

EXOSC10 expression in the mouse epididymis

To investigate the function of EXOSC10 in mouse epididymis, we first analyzed its mRNA expression levels in different tissues of adult mice by RT-qPCR. The results showed that *Exosc10*

https://doi.org/10.1017/S0967199424000418 Published online by Cambridge University Press

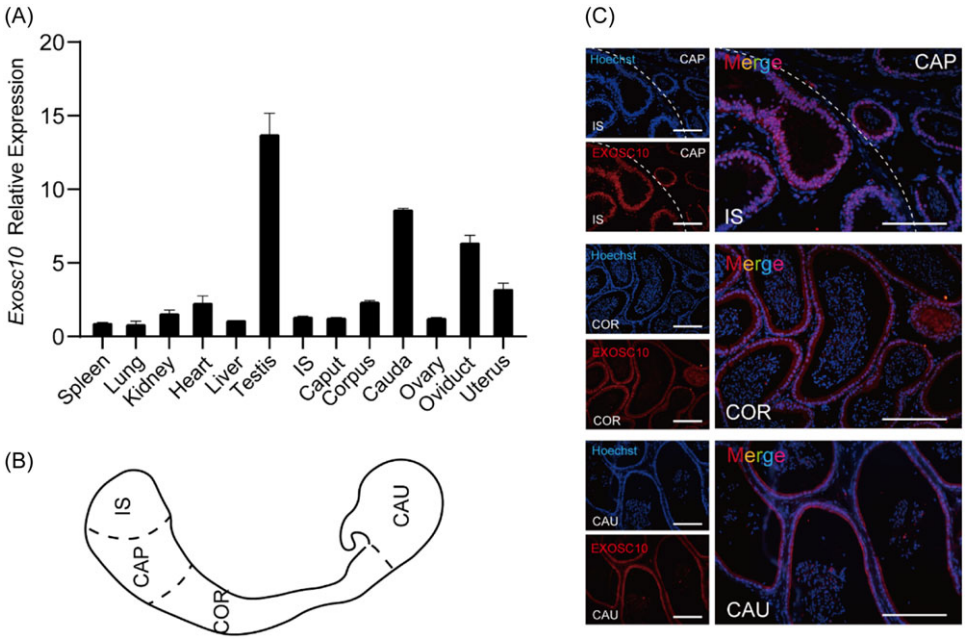

Figure 1. Expression pattern of EXOSC10 in mouse epididymis. (A) RT-qPCR analysis of *Exosc10* mRNA expression in various organs of adult mice. *Exosc10* is widely expressed in different organs, including the testis and epididymis. The expression level of *Exosc10* in the spleen relative to *β-actin* was set to 1. Data are presented as mean ± SD for n = 3 biologically independent experiments. (B) Schematic diagram of mouse epididymis, including the IS, CAP, COR, and CAU. (C) Immunofluorescence staining of EXOSC10 (red) and DNA (blue) in adult epididymis. Scale bar, 50 μm. Representative of n = 3 independent biological replicates with similar results per condition. IS, initial segment; CAP, Caput; COR, Corpus; CAU, Cauda.

expressed ubiquitously in mice, including epididymis (Figure 1A). As epididymis is further subdivided into IS, CAP, COR, and CAU (Figure 1B), we performed the immunofluorescence staining of the entire epididymis and found that EXOSC10 was localized in the epithelial cells of the different segments of the epididymis (Figure 1C). Together, these results indicated that EXOSC10 was expressed in the mouse epididymis epithelium.

Generation of Exosc10 cKO mice

To elucidate the role of EXOSC10 during epithelial cell differentiation in the IS, we established an *Exosc10* cKO model by crossing *Exosc10*$^{F/F}$ mice with *Lcn9-Cre* knock-in mice which expressed CRE recombinase, primarily in the principal cells of the IS as early as at post-natal day 17 (P17). *Exosc10* exons 4, 5, and 6 flanked with LoxP sites were excised after crossing with *Lcn9-Cre* mice (Figure 2A). After three generations of breeding (Figure 2B), we obtained control and *Exosc10* cKO mice and performed genomic PCR for genotypic analysis (Figure 2C). The *Exosc10* mRNA and EXOSC10 levels were significantly reduced in the IS of *Exosc10* cKO mice compared with those in the control mice as estimated by RT-qPCR and immunoblot assay, respectively (Figure 2D–F). Moreover, the results of the immunofluorescence staining demonstrated that EXOSC10 was absent in the principal cells of the IS but present in other cell types of *Exosc10* cKO mice (Figure 2G). Collectively, these results indicated that EXOSC10 was successfully ablated in the principal cells of the IS in *Exosc10* cKO mice.

Morphology of testis and epididymis in Exosc10 cKO mice

The effects of EXOSC10 on the testis and epididymis were examined by analyzing their morphology in *Exosc10* cKO mice. The results revealed no significant differences in the size and weight of the testis and epididymis in 3-month-old *Exosc10* cKO mice compared with the controls (Figure 3A–D). Moreover, the H&E staining of the testis and epididymis showed no obvious anomalies with normal spermatogenesis even in the absence of EXOSC10 (Figure 3E). In addition, epithelial cells of the IS and other segments, including CAP, COR, and CAU displayed normal histology in *Exosc10* cKO mice (Figure 3F). Besides, the numbers of spermatozoa in CAP, COR, and CAU were comparable between control and *Exosc10* cKO mice (Figure 3F). These results indicated that *Exosc10* deficiency in the IS did not affect spermatogenesis and epididymal development.

Sperm morphology and motility of Exosc10 cKO mice

IS of epididymis synthesizes and secretes a set of proteins to provide a unique luminal environment required for sperm maturation. First, no significant difference was observed in the sperm counts in the cauda epididymis of control and *Exosc10* cKO mice (Figure 4A). Next, results of H&E staining revealed a normal morphology of most sperm (~80%) in both control and *Exosc10* cKO mice and only ~20% abnormal sperm in *Exosc10* cKO mice relative to the control males (Figure 4B, C). This indicated that *Exosc10* cKO did not affect sperm concentration and morphology. Furthermore, sperm motility was analyzed using CASA and the results demonstrated no significant differences in cauda sperm motility and progressive motility (Figure 4D, E). Nevertheless, sperm parameters, including straight line velocity (VSL), curvilinear velocity (VCL), average path velocity (VAP), and amplitude of lateral head displacement (ALH) after 10 min (or 120 min) of incubation remained unaffected in the absence of EXOSC10 (Figure 4F–I). These data suggested that sperm motility was not affected after EXOSC10 ablation in the IS.

Sperm acrosome reaction in Exosc10 cKO mice

Acrosome exocytosis during fertilization releases lytic enzymes to facilitate sperm passage through the cumulus cells and zona pellucida of the eggs; therefore, the integrity of the acrosome is an important indicator of sperm quality. The frequency of acrosome exocytosis was estimated by staining cauda sperm with PNA and calculating the ratio of spontaneous acrosome reaction. The results revealed that the rates of spontaneous acrosome reaction in non-capacitated and capacitated conditions were comparable between control and *Exosc10* cKO mice (Figure 5A–C), indicating a normal sperm acrosome reaction frequency in *Exosc10* cKO mice.

https://doi.org/10.1017/S0967199424000418 Published online by Cambridge University Press

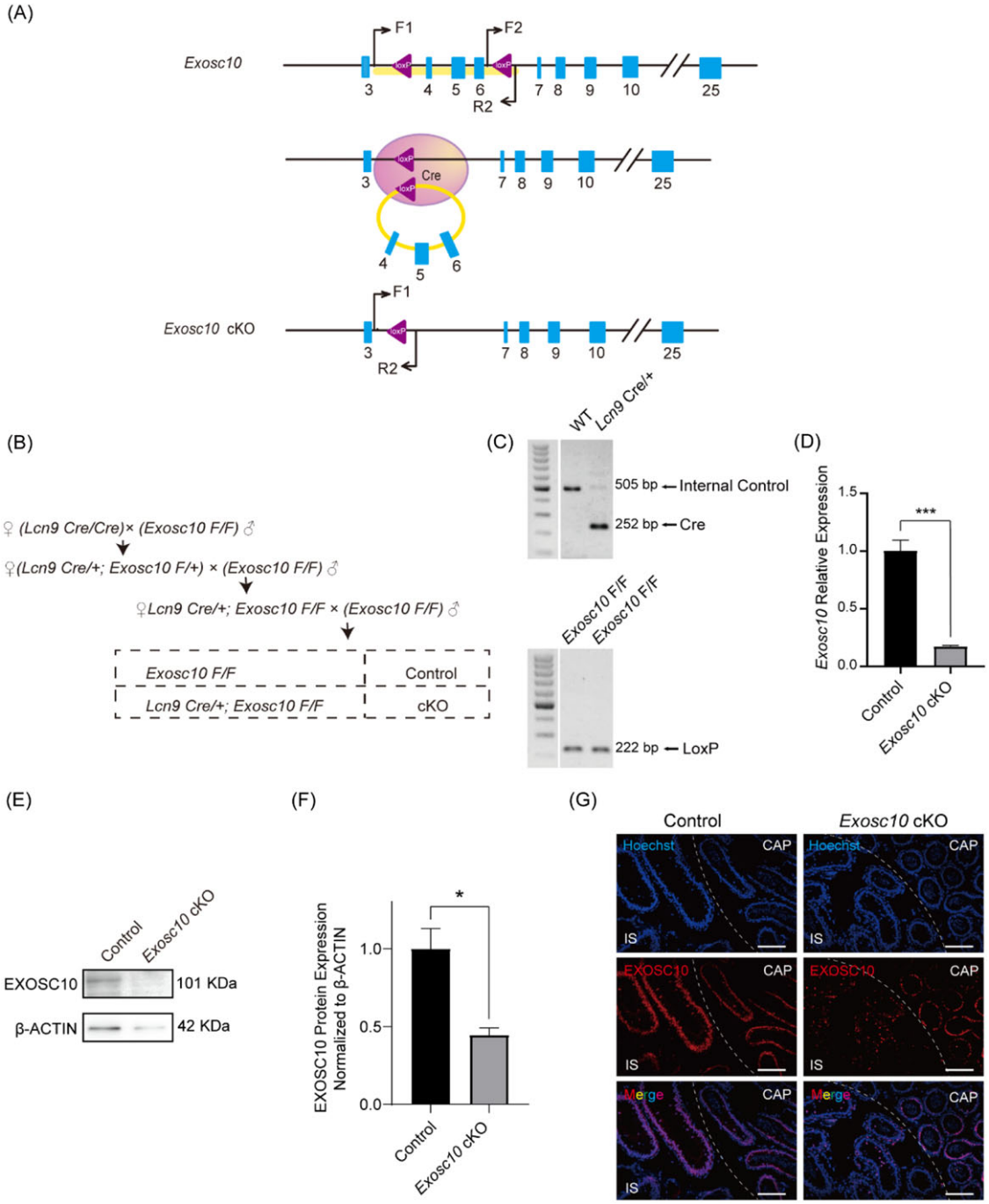

Figure 2. Generation of *Exosc10* cKO mice with *Lcn9-Cre*. (A) Schematic diagram of targeting strategy for generation of *Exosc10* cKO mice. Exons 4, 5, and 6 were deleted upon CRE-mediated recombination. (B) The schematic diagram of breeding strategies to obtain *Exosc10* cKO mice. (C) Genomic PCR genotyping to detect LoxP band (222 bp) and Cre band (252 bp). (D) *Exosc10* mRNA expression levels in the initial segment of adult control and *Exosc10* cKO mice. The expression level of *Exosc10* in control relative to *β-actin* was set to 1. Data are presented as mean ± SD for n = 3 biologically independent experiments. ***$P < 0.001$. (E) Western blotting depicting the levels of EXOSC10 in the initial segment of control and *Exosc10* cKO mice. Representative of n = 3 independent biological replicates with similar results per condition. (F) Quantification of EXOSC10 protein levels in the initial segment of control and *Exosc10* cKO mice. *$P < 0.05$ (G) Immunofluorescence staining of EXOSC10 in the initial segment of control and *Exosc10* cKO mice. DNA was stained with Hoechst 33342. Scale bar, 50 μm. Representative of n = 3 independent biological replicates with similar results per condition.

Alterations of IS differentiation-related genes in Exosc10 cKO mice

To determine the effect of EXOSC10 unavailability on the transcriptome of IS, a set of genes associated with IS differentiation was analyzed by RT-qPCR. The results indicated that most of the gene expression levels remained unaffected, including *Pten*, *Ros1*, *Mst1*, *Src*, and *Esr1*. While the expression levels of *Mst2* and *Ar* were slightly increased, those of *Dicer1* and *Esr2* were somewhat decreased (Figure 6A–I). Although the levels were statistically different for all four genes, the change was less than 1.5-fold. These data suggested that the loss of EXOSC10 had no significant influence on the IS transcriptome in *Exosc10* cKO mice.

https://doi.org/10.1017/S0967199424000418 Published online by Cambridge University Press

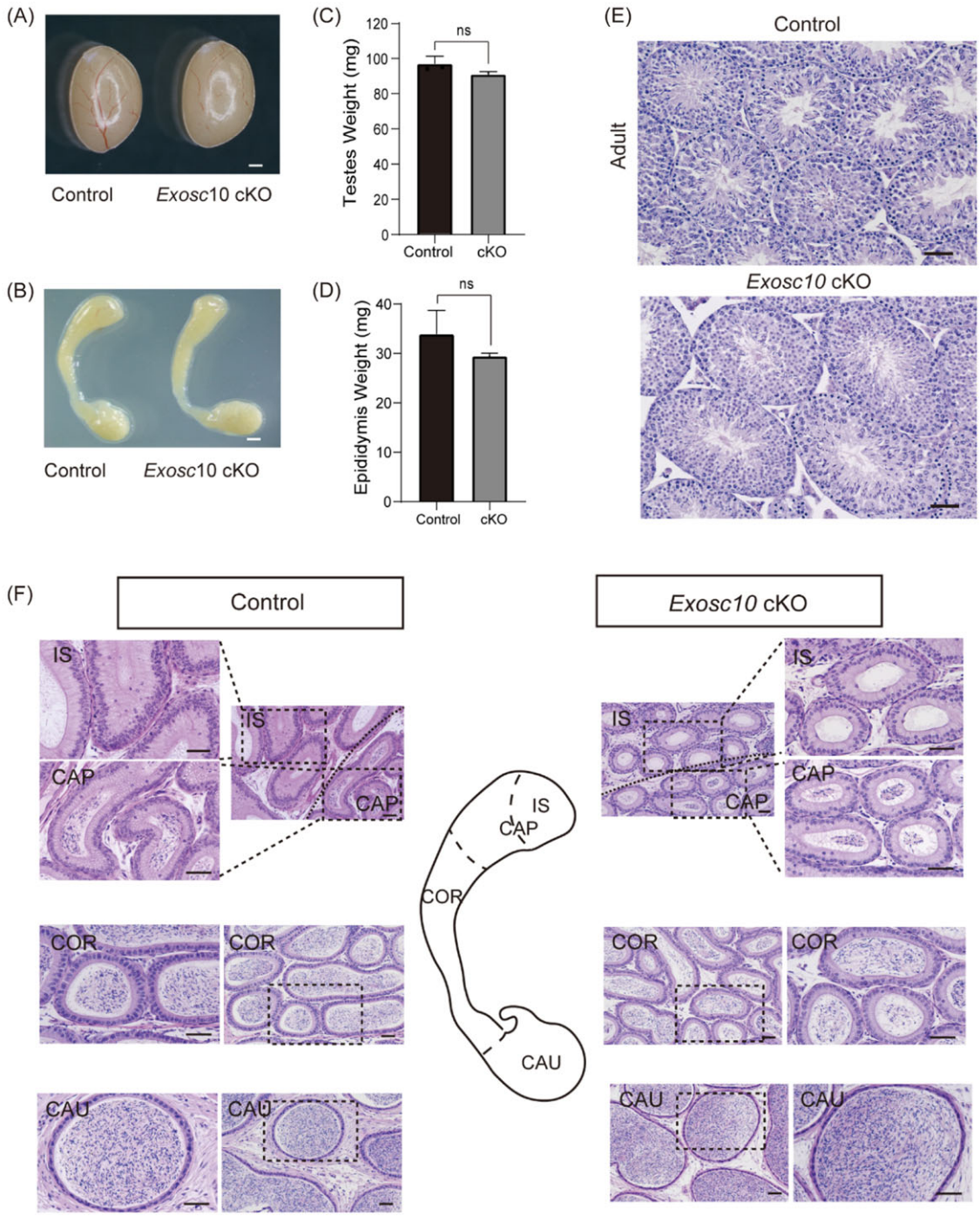

Figure 3. Histological analysis of testis and epididymis in adult *Exosc10* cKO mice. (A, B) Morphology of 3-month-old testis and epididymis of control and *Exosc10* cKO mice. (C, D) Histograms of testis and epididymis weights from control and *Exosc10* cKO mice. Mean ± SD for n = 3 biologically independent samples from 3 different animals. ns, no significance. (E) H&E staining of testes from control and *Exosc10* cKO mice. Scale bar, 50 μm. (F) H&E staining of different segments of epididymis from control and *Exosc10* cKO mice, including initial segment (IS), Caput (CAP), Corpus (COR), and Cauda (CAU). Scale bar, 50 μm. Representative of n = 3 (E, F) independent biological replicates with similar results per condition.

Fertility of Exosc10 cKO male mice

The adult control or *Exosc10* cKO male mice mated with the wild-type female mice for at least 3 months and male fertility was assessed. The results showed that *Exosc10* cKO males had nearly the same number of pups per litter as control males (Figure 7). This indicated that EXOSC10 in the IS was not essential for male fertility.

Discussion

Previous studies have reported that epididymal aging occurs in a segment-dependent manner and the proximal epididymis is particularly vulnerable due to rich blood supply (Huang *et al.*, 2021; Markey and Meyer 1992). IS is the initial part of the epididymis and its dysfunction may cause sperm maturation defects and male infertility (Kiyozumi *et al.*, 2020; Krutskikh *et al.*,

https://doi.org/10.1017/S0967199424000418 Published online by Cambridge University Press

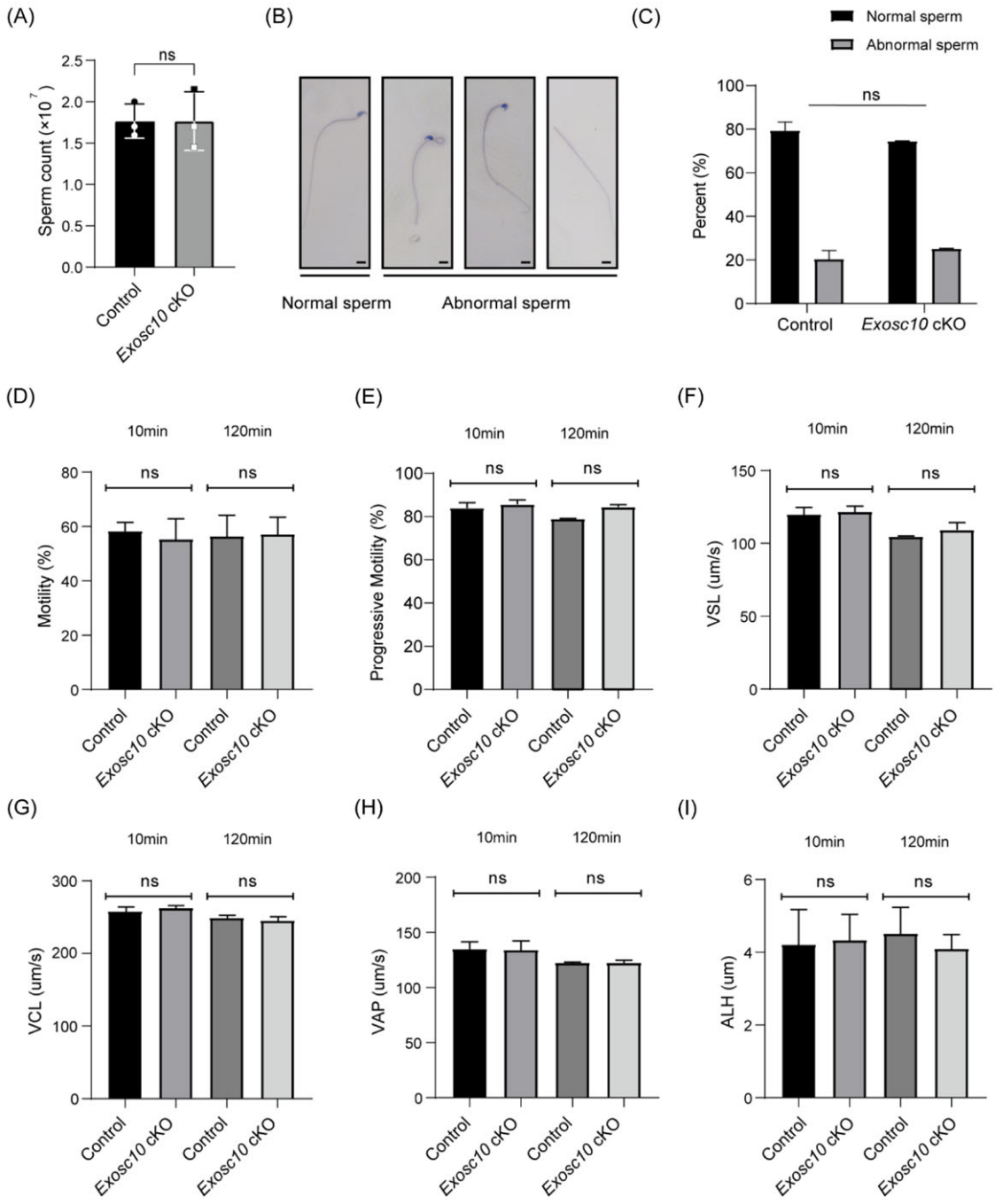

Figure 4. Sperm morphology and motility in control and *Exosc10* cKO mice. (A) Sperm counts of cauda epididymis from control and *Exosc10* cKO mice. (B) H&E staining of sperm from cauda epididymis of control and *Exosc10* cKO mice. Scale bar, 10 μm. (C) The percentage of normal and abnormal sperm from cauda epididymis of control and *Exosc10* cKO mice. CASA analysis of (D) sperm motility, (E) progressive motility, (F) VSL, straight-line velocity, (G) VCL, curvilinear velocity, (H) VAP, average path velocity, and (I) ALH, amplitude of lateral head displacement. Data are presented as mean ± SD for n = 3 biologically independent experiments. ns, no significance.

2011; Murashima *et al.*, 2011; O'Hara *et al.*, 2011; Sonnenberg-Riethmacher *et al.*, 1996). These findings suggest that IS plays a critical role during sperm transition and maturation in the epididymis. Therefore, our study focused on the development and function of IS in the mouse epididymis.

The effects of various IS genes on sperm maturation and male fertility have been characterized. *Ros1* KO males show sperm maturation defects and sterility due to the disruption of IS formation (Sonnenberg-Riethmacher *et al.*, 1996). *Lgr4* mutant males are completely infertile with immotile cauda sperm due to defects in post-natal epididymal coiling and IS differentiation (Hoshii *et al.*, 2007; Mendive *et al.*, 2006). Moreover, androgen receptor (*Ar*) KO mice display a sperm transition defect and accumulation of spermatozoa in the efferent ducts, which suggests the importance of epididymal androgen signaling in IS formation and principal cell differentiation (Murashima *et al.*, 2011; O'Hara *et al.*, 2011). Similarly, *Dicer1* ablation in the epididymis causes dedifferentiation of the epithelium and imbalanced sex steroid signaling (Bjorkgren *et al.*, 2012). Besides, OVCH2, a secreted protease, is exquisitely localized to the IS of the epididymis and its

https://doi.org/10.1017/S0967199424000418 Published online by Cambridge University Press

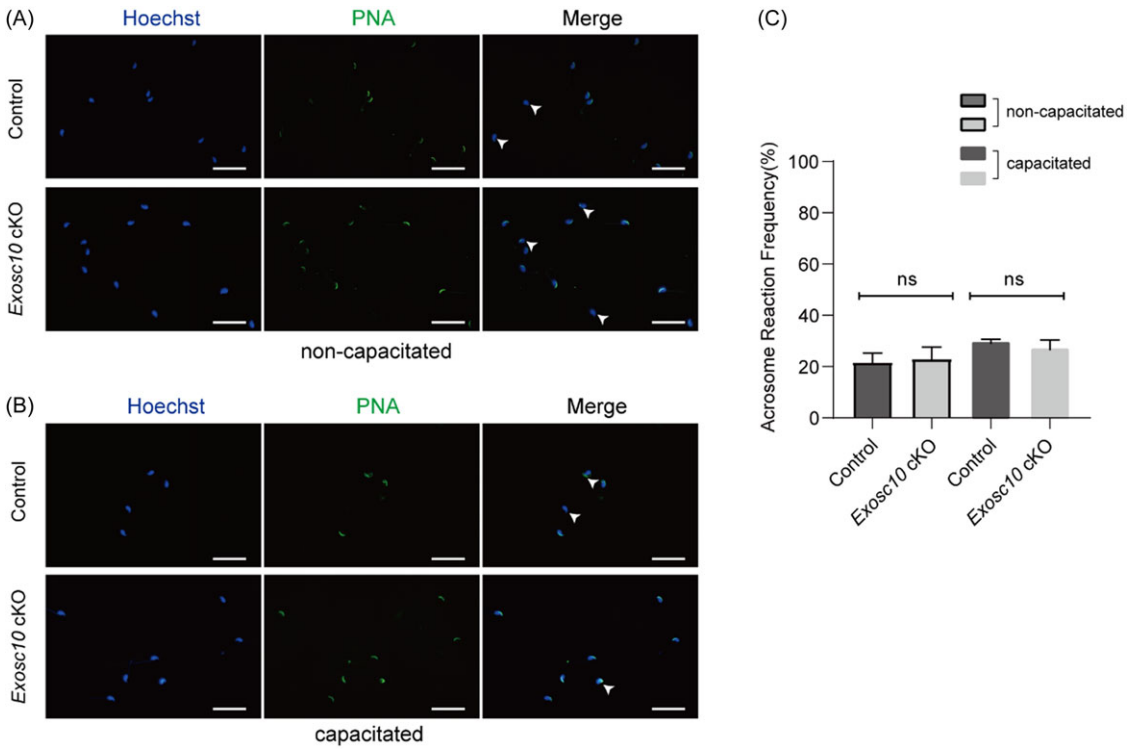

Figure 5. Frequency of sperm acrosome reaction in control and *Exosc10* cKO mice. (A, B) Representative images of sperm acrosome reaction in control and *Exosc10* cKO mice in non-capacitated (A) and capacitated (B) conditions. Sperm acrosome was labeled by PNA. DNA was stained with Hoechst 33342. White arrowheads, incomplete acrosomes. Scale bar, 50 μm. Representative of n = 3 independent biological replicates with similar results per condition. (C) The frequency of spontaneous acrosome reaction in non-capacitated or capacitated sperm. Data are presented as mean ± SD for n = 3 biologically independent experiments. ns, no significance.

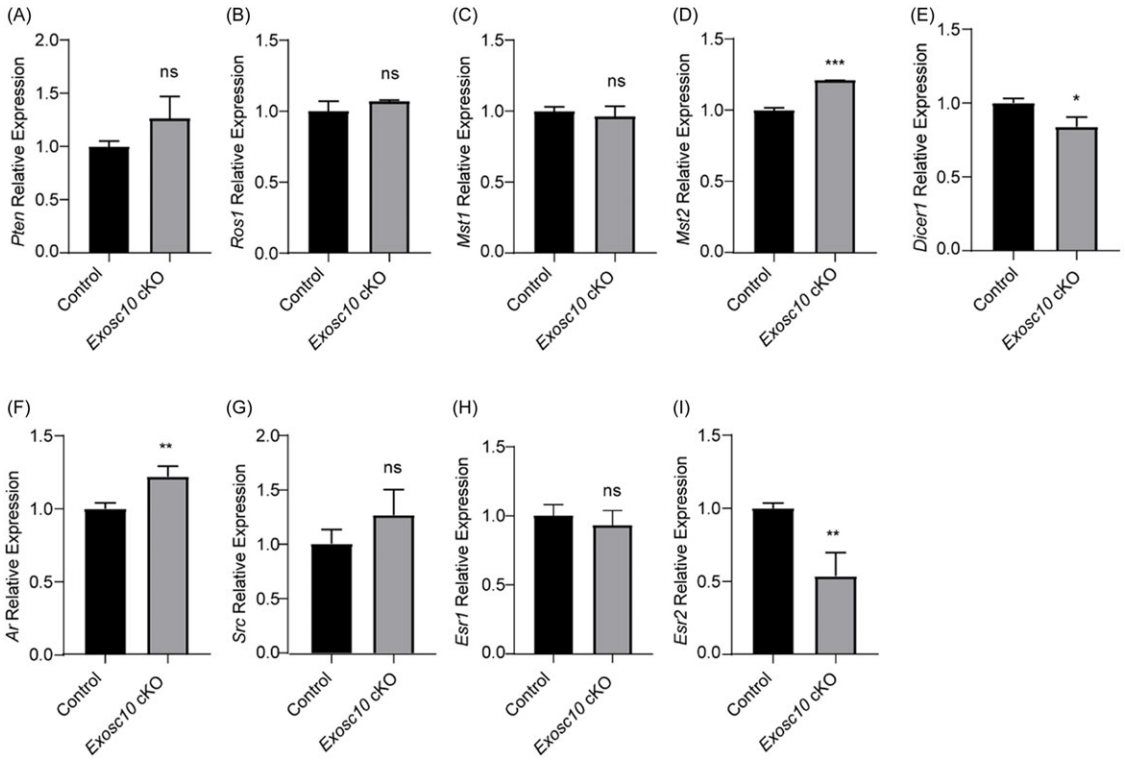

Figure 6. Relative expression levels of differentiation-related genes in the initial segment. RT-qPCR analysis of (A) *Pten*, (B) *Ros1*, (C) *Mst1*, (D) *Mst2*, (E) *Dicer1*, (F) *Ar*, (G) *Src*, (H) *Esr1*, and (I) *Esr2* in control and *Exosc10* cKO mice. The expression levels of genes in control relative to *β-actin* were set to 1. Data are presented as mean ± SD for n = 3 biologically independent experiments; $^{*}P < 0.05$, $^{**}P < 0.01$, $^{***}P < 0.001$, ns, no significance.

https://doi.org/10.1017/S0967199424000418 Published online by Cambridge University Press

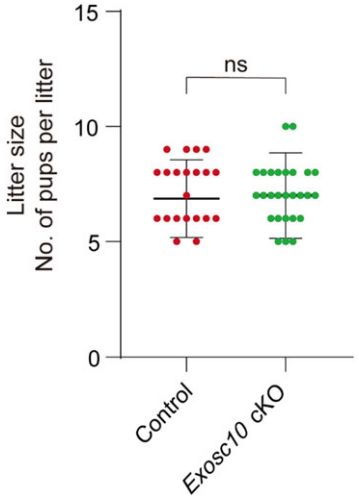

Figure 7. Fertility test of *Exosc10* cKO male mice. Each male mouse mated with one wild-type female mouse for at least 3 months (n = 3 per genotype). The number of pups per litter was recorded. Data are presented as mean ± SD; ns, no significance.

absence causes sperm defects, including aberrant ADAM3 processing, inability to bind to the zona pellucida, and passage through the utero-tubal junction (Kiyozumi *et al.*, 2020).

Recent studies have shown that EXOSC10 is involved in the regulation of gamete and embryonic development in mice. *Exosc10* inactivation in the oocytes using *Gdf9-Cre* impairs oocyte development and maturation, leading to a depleted ovarian reserve (Demini *et al.*, 2023). Moreover, the deletion of *Exosc10* in the oocytes using *Zp3-Cre* causes female subfertility due to delayed germinal vesicle breakdown (Wu and Dean 2020). In addition, conditional disruption of *Exosc10* in male germ cells using *Ddx4-Cre* or *Stra8-Cre* impairs the growth and development of germ cells (Jamin *et al.*, 2017). According to another study, *Exosc10* (−/−) mutant embryos are arrested at the eight-cell embryo/morula transition stage (Petit *et al.*, 2022). To further investigate whether EXOSC10 is required for IS differentiation and sperm maturation, we established an *Exosc10* cKO mouse model using *Lcn9-Cre* knock-in mice which expressed CRE enzyme in the principal cells of the IS as early as at P17 (Gong *et al.*, 2021). Unexpectedly, *Exosc10* cKO males showed normal spermatogenesis, IS development, sperm morphology, motility, and fertility. Moreover, we examined a set of IS differentiation-related genes and found that *Exosc10* deficiency had no significant effect on the transcriptome levels. Only *Mst2*, *Dicer1*, *Ar*, and *Esr2* mRNA levels were slightly modulated in the absence of EXOSC10. Consequently, our findings suggest that EXOSC10 is dispensable for IS differentiation.

The *Lcn9-Cre*-mediated EXOSC10 deletion occurs only in the principal cells of the IS in the entire epididymis. It is speculated that deletion of a large part of the epididymis or other cell types may affect the phenotype and fertility. Some other *Cre* lines, such as *Defb41-Cre* and *Cyp17a1-Cre*, express recombinase in the epithelium of the most proximal part of the epididymis (IS and CAP) and epithelial cells of the epididymis, respectively (Bjorkgren *et al.*, 2012; Gannon *et al.*, 2022); therefore, they may be used to explore the potential function of EXOSC10 in the development of epididymis and sperm maturation. In conclusion, our findings suggest that *Exosc10* deficiency in the IS is dispensable for epididymal differentiation, sperm maturation, and male fertility.

Supplementary material. The supplementary material for this article can be found at https://doi.org/10.1017/S0967199424000418

Acknowledgments. We thank Bullet Edits for the English language editing of the manuscript. The authors are grateful to Professor You-Qiang Su from the School of Life Sciences, Shandong University for providing his lab facilities, and Professor Xiao-Yang Sun from the School of Life Sciences, Shandong University for providing *Lcn9-Cre* mice.

Author contributions. N. Li., and Z. Wang. designed the experiments. M. Zhou., J. Yu., Y. Xu., H. Li., YQ. Feng., X. Wang., and F. Qiu. performed the experiments. M. Zhou., N. Li., and Z. Wang. analyzed the data. M. Zhou., and Z. Wang. wrote the paper.

Competing interests. None.

Funding. This work was supported by grants from the National Natural Science Foundation of China (NSFC 32370904); the Shandong Excellent Young Scientists Fund Program (Overseas), grant number 2022HWYQ-026; the Natural Science Foundation of Shandong Province, grant number ZR2022MC005; the Qilu Scholarship of Shandong University, grant number 61200082163142.

Ethical standards. This study was carried out in the guidelines of the School of Life Sciences, Shandong University, China.

References

Bjorkgren I, Saastamoinen L, Krutskikh A, Huhtaniemi I, Poutanen M and Sipila P (2012) Dicer1 ablation in the mouse epididymis causes dedifferentiation of the epithelium and imbalance in sex steroid signaling. *PLoS One* **7**(6), e38457. https://doi.org/10.1371/journal.pone.0038457.

Cornwall GA (2009) New insights into epididymal biology and function. *Human Reproduction Update* **15**(2), 213–227. https://doi.org/10.1093/humupd/dmn055.

Cosentino MJ and Cockett AT (1986) Structure and function of the epididymis. *Urological Research* **14**(5), 229–240. https://doi.org/10.1007/BF00256565.

Demini L, Kervarrec C, Guillot L, Com E, Lavigne R, Kernanec PY, Primig M, Pineau C, Petit FG and Jamin SP (2023) Inactivation of Exosc10 in the oocyte impairs oocyte development and maturation, leading to a depletion of the ovarian reserve in mice. *International Journal of Biological Sciences* **19**(4), 1080–1093. https://doi.org/10.7150/ijbs.72889.

Dube E, Chan PT, Hermo L and Cyr DG (2007) Gene expression profiling and its relevance to the blood-epididymal barrier in the human epididymis. *Biology of Reproduction* **76**(6), 1034–1044. https://doi.org/10.1095/biolreprod.106.059246.

Elbashir S, Magdi Y, Rashed A, Henkel R and Agarwal A (2021) Epididymal contribution to male infertility: An overlooked problem. *Andrologia* **53**(1), e13721. https://doi.org/10.1111/and.13721.

Gannon AL, Darbey AL, Chensee G, Lawrence BM, O'Donnell L, Kelso J, Reed N, Parameswaran S, Smith S, Smith LB and Rebourcet D (2022) A novel model using AAV9-Cre to knockout adult leydig cell gene expression reveals a physiological role of glucocorticoid receptor signalling in leydig cell function. *International Journal of Molecular Sciences* **23**(23), 15015. https://doi.org/10.3390/ijms232315015.

Gong QQ, Wang X, Dou ZL, Zhang KY, Liu XG, Gao JG and Sun XY (2021) A novel mouse line with epididymal initial segment-specific expression of Cre recombinase driven by the endogenous Lcn9 promoter. *PLoS One* **16**(7), e0254802. https://doi.org/10.1371/journal.pone.0254802.

Hartley JL, Zachos NC, Dawood B, Donowitz M, Forman J, Pollitt RJ, Morgan NV, Tee L, Gissen P, Kahr WH, Knisely AS, Watson S, Chitayat D, Booth IW, Protheroe S, Murphy S, de Vries E, Kelly DA and Maher ER (2010) Mutations in TTC37 cause trichohepatoenteric syndrome (phenotypic diarrhea of infancy). *Gastroenterology* **138**(7), 2388–2398, 2398.e2381-2382. https://doi.org/10.1053/j.gastro.2010.02.010.

Hoshii T, Takeo T, Nakagata N, Takeya M, Araki K and Yamamura K (2007) LGR4 regulates the postnatal development and integrity of male

reproductive tracts in mice. *Biology of Reproduction* **76**(2), 303–313. https://doi.org/10.1095/biolreprod.106.054619.

Huang Y, Li X, Sun X, Yao J, Gao F, Wang Z, Hu J, Wang Z, Ouyang B, Tu X, Zou X, Liu W, Lu M, Deng C, Yang Q and Xie Y (2021) Anatomical transcriptome atlas of the male mouse reproductive system during aging. *Frontiers in Cell and Developmental Biology* **9**, 782824. https://doi.org/10.3389/fcell.2021.782824.

James ER, Carrell DT, Aston KI, Jenkins TG, Yeste M and Salas-Huetos A (2020) The role of the epididymis and the contribution of epididymosomes to mammalian reproduction. *International Journal of Molecular Sciences* **21**(15), 5377. https://doi.org/10.3390/ijms21155377.

Jamin SP, Petit FG, Kervarrec C, Smagulova F, Illner D, Scherthan H and Primig M (2017) EXOSC10/Rrp6 is post-translationally regulated in male germ cells and controls the onset of spermatogenesis. *Scientific Reports* **7**(1), 15065. https://doi.org/10.1038/s41598-017-14643-y.

Johnston DS, Jelinsky SA, Bang HJ, DiCandeloro P, Wilson E, Kopf GS and Turner TT (2005) The mouse epididymal transcriptome: transcriptional profiling of segmental gene expression in the epididymis. *Biology of Reproduction* **73**(3), 404–413. https://doi.org/10.1095/biolreprod.105.039719.

Joseph A, Shur BD and Hess RA (2011) Estrogen, efferent ductules, and the epididymis. *Biology of Reproduction* **84**(2), 207–217. https://doi.org/10.1095/biolreprod.110.087353.

Kiyozumi D, Noda T, Yamaguchi R, Tobita T, Matsumura T, Shimada K, Kodani M, Kohda T, Fujihara Y, Ozawa M, Yu Z, Miklossy G, Bohren KM, Horie M, Okabe M, Matzuk MM and Ikawa M (2020) NELL2-mediated lumicrine signaling through OVCH2 is required for male fertility. *Science* **368**(6495), 1132–1135. https://doi.org/10.1126/science.aay5134.

Knight JR, Bastide A, Peretti D, Roobol A, Roobol J, Mallucci GR, Smales CM and Willis AE (2016) Cooling-induced SUMOylation of EXOSC10 down-regulates ribosome biogenesis. *RNA* **22**(4), 623–635. https://doi.org/10.1261/rna.054411.115.

Krutskikh A, De Gendt K, Sharp V, Verhoeven G, Poutanen M and Huhtaniemi I (2011) Targeted inactivation of the androgen receptor gene in murine proximal epididymis causes epithelial hypotrophy and obstructive azoospermia. *Endocrinology* **152**(2), 689–696. https://doi.org/10.1210/en.2010-0768.

Livak KJ and Schmittgen TD (2001) Analysis of relative gene expression data using real-time quantitative PCR and the 2(-Delta Delta C(T)) Method. *Methods* **25**(4), 402–408. https://doi.org/10.1006/meth.2001.1262.

Markey CM and Meyer GT (1992) A quantitative description of the epididymis and its microvasculature: an age-related study in the rat. *Journal of Anatomy* **180** (Pt 2)(Pt 2), 255–262.

Martinez-Garcia F, Regadera J, Cobo P, Palacios J, Paniagua R and Nistal M (1995) The apical mitochondria-rich cells of the mammalian epididymis. *Andrologia* **27**(4), 195–206. https://doi.org/10.1111/j.1439-0272.1995.tb01093.x.

Mendive F, Laurent P, Van Schoore G, Skarnes W, Pochet R and Vassart G (2006) Defective postnatal development of the male reproductive tract in LGR4 knockout mice. *Developmental Biology* **290**(2), 421–434. https://doi.org/10.1016/j.ydbio.2005.11.043.

Murashima A, Miyagawa S, Ogino Y, Nishida-Fukuda H, Araki K, Matsumoto T, Kaneko T, Yoshinaga K, Yamamura K, Kurita T, Kato S, Moon AM and Yamada G (2011) Essential roles of androgen signaling in Wolffian duct stabilization and epididymal cell differentiation. *Endocrinology* **152**(4), 1640–1651. https://doi.org/10.1210/en.2010-1121.

O'Hara L, Welsh M, Saunders PT and Smith LB (2011) Androgen receptor expression in the caput epididymal epithelium is essential for development of the initial segment and epididymal spermatozoa transit. *Endocrinology* **152**(2), 718–729. https://doi.org/10.1210/en.2010-0928.

Pefanis E, Wang J, Rothschild G, Lim J, Kazadi D, Sun J, Federation A, Chao J, Elliott O, Liu ZP, Economides AN, Bradner JE, Rabadan R and Basu U (2015) RNA exosome-regulated long non-coding RNA transcription controls super-enhancer activity. *Cell* **161**(4), 774–789. https://doi.org/10.1016/j.cell.2015.04.034.

Petit FG, Jamin SP, Kernanec PY, Becker E, Halet G and Primig M (2022) EXOSC10/Rrp6 is essential for the eight-cell embryo/morula transition. *Developmental Biology* **483**, 58–65. https://doi.org/10.1016/j.ydbio.2021.12.010.

Rudnik-Schöneborn S, Senderek J, Jen JC, Houge G, Seeman P, Puchmajerová A, Graul-Neumann L, Seidel U, Korinthenberg R, Kirschner J, Seeger J, Ryan MM, Muntoni F, Steinlin M, Sztriha L, Colomer J, Hübner C, Brockmann K, Van Maldergem L, Schiff M, Holzinger A, Barth P, Reardon W, Yourshaw M, Nelson SF, Eggermann T and Zerres K (2013) Pontocerebellar hypoplasia type 1: clinical spectrum and relevance of EXOSC3 mutations. *Neurology* **80**(5), 438–446. https://doi.org/10.1212/WNL.0b013e31827f0f66.

Sipila P, Cooper TG, Yeung CH, Mustonen M, Penttinen J, Drevet J, Huhtaniemi I and Poutanen M (2002) Epididymal dysfunction initiated by the expression of simian virus 40 T-antigen leads to angulated sperm flagella and infertility in transgenic mice. *Molecular Endocrinology* **16**(11), 2603–2617. https://doi.org/10.1210/me.2002-0100.

Sonnenberg-Riethmacher E, Walter B, Riethmacher D, Godecke S and Birchmeier C (1996) The c-ros tyrosine kinase receptor controls regionalization and differentiation of epithelial cells in the epididymis. *Genes & Development* **10**(10), 1184–1193. https://doi.org/10.1101/gad.10.10.1184.

Sullivan R, Legare C, Lamontagne-Proulx J, Breton S and Soulet D (2019) Revisiting structure/functions of the human epididymis. *Andrology* **7**(5), 748–757. https://doi.org/10.1111/andr.12633.

Thimon V, Koukoui O, Calvo E and Sullivan R (2007) Region-specific gene expression profiling along the human epididymis. *Molecular Human Reproduction* **13**(10), 691–704. https://doi.org/10.1093/molehr/gam051.

van Dijk EL, Schilders G and Pruijn GJ (2007) Human cell growth requires a functional cytoplasmic exosome, which is involved in various mRNA decay pathways. *RNA* **13**(7), 1027–1035. https://doi.org/10.1261/rna.575107.

Weißbach S, Langer C, Puppe B, Nedeva T, Bach E, Kull M, Bargou R, Einsele H, Rosenwald A, Knop S and Leich E (2015) The molecular spectrum and clinical impact of DIS3 mutations in multiple myeloma. *British Journal of Haematology* **169**(1), 57–70. https://doi.org/10.1111/bjh.13256.

Wu D and Dean J (2020) EXOSC10 sculpts the transcriptome during the growth-to-maturation transition in mouse oocytes. *Nucleic Acids Research* **48**(10), 5349–5365. https://doi.org/10.1093/nar/gkaa249.

Zhou W, De Iuliis GN, Dun MD and Nixon B (2018) Characteristics of the epididymal luminal environment responsible for sperm maturation and storage. *Frontiers in Endocrinology* **9**, 59. https://doi.org/10.3389/fendo.2018.00059.

https://doi.org/10.1017/S0967199424000418 Published online by Cambridge University Press